HHS Public Access

Author manuscript

Eur J Anat. Author manuscript; available in PMC 2015 May 04.

Published in final edited form as:

Eur J Anat. 2015 January 1; 19(1): 49–56.

Elliptical Morphology of the Carpal Tunnel Cross Section

Joseph N. Gabra[1,2], **Dong Hee Kim**[1], and **Zong-Ming Li**[1,2,*]

[1]Hand Research Laboratory, Departments of Biomedical Engineering, Orthopaedic Surgery, and Physical Medicine and Rehabilitation, Cleveland Clinic, Cleveland, Ohio

[2]Department of Chemical and Biomedical Engineering, Cleveland State University, Cleveland, OH

Summary

Although the carpal tunnel is known for its anatomical constituents, its morphology is not well recognized. The aim of this study was to investigate the morphometric properties of the carpal tunnel and its surrounding structures. Magnetic resonance, cross-sectional images of the distal carpal tunnel were collected from eight cadaveric hands. Morphological analyses were performed for the cross sections of the carpal tunnel, interior carpus boundary, and exterior carpus boundary. The specimens had a carpal arch width and height of 23.9 ± 2.9 mm and 2.2 ± 0.9 mm, respectively. The carpal tunnel, interior carpus boundary, and exterior carpus boundary had perimeters of 54.8 ± 4.5 mm, 68.5 ± 7.0 mm, and 130.6 ± 11.8 mm, respectively, and areas of 183.5 ± 30.1 mm^2, 240.7 ± 40.2 mm^2, and 1002.3 ± 183.7 mm^2, respectively. The cross sections were characterized by elliptical fitting with aspect ratios of 1.96 ± 0.15, 1.96 ± 0.19, and 1.76 ± 0.19 for the carpal tunnel, interior carpus boundary, and exterior carpus boundary, respectively. The major axis of the boundaries increased in pronation angle, relative to the hamate-trapezium axis, for the exterior carpus (6.0 ± 3.0°), interior carpus (8.2 ± 3.2°), and carpal tunnel (15.9 ± 2.2°). This study advances our understanding of the structural anatomy of the carpal tunnel, and the morphological information is valuable in the identification of structural abnormality, assistance of surgical planning, and evaluation of treatment of effects.

Keywords

carpal tunnel; carpus; morphology

2 Introduction

The carpal tunnel is a compartment within the wrist that contains nine flexor tendons and the median nerve. The volar border of the carpal tunnel is bounded by the transverse carpal ligament (TCL), and the remaining border is formed by carpal bones connected by intercarpal ligaments. Although wrist anatomy is known for its constituents, the morphological properties of the carpal tunnel structure are not well recognized.

[*]**Correspondence**. Zong-Ming Li, PhD, Cleveland Clinic, 9500 Euclid Avenue, ND20, Cleveland, OH 44195, Phone: (216) 444-1211, Fax: (216) 444-9198, liz4@ccf.org.

Carpal tunnel morphometry provides useful anatomical information to screen at risk populations for carpal tunnel pathologies, determine aberrant changes to the carpal tunnel and its contents, aid in surgical planning, and evaluate surgical effects. For example, studies have found correlations between anthropometry and morphometry of the hand and wrist with median nerve latency and even carpal tunnel syndrome (Bleecker et al., 1985, Chroni et al., 2001, Gordon et al., 1988, Kamolz et al., 2004, Radecki, 1994). Morphometry of the carpal tunnel has also been used to evaluate the extent of median nerve compression (Brahme et al., 1997, Buchberger et al., 1991, Buchberger et al., 1992, Kamolz et al., 2004, Lee et al., 2005, Lee et al., 1999, Mesgarzadeh et al., 1989b, Zagnoli et al., 1999). Other studies have linked median nerve compression with TCL palmar bowing (Mesgarzadeh et al., 1989b) and carpal tunnel stenosis (Dekel et al., 1980, Healy et al., 1990, Papaioannou et al., 1992). For surgical planning, the carpal tunnel depth can indicate the technique needed for carpal tunnel release (Kamolz et al., 2001). Lastly, carpal tunnel release has been shown to change carpal tunnel morphology (Ablove et al., 1994, Cho et al., 2008, Kato et al., 1994, Kim et al., 2013, Lee et al., 2005, Richman et al., 1989).

Although carpal tunnel morphometry is useful for many purposes there are some limitations in how it is currently utilized. For example, some studies have evaluated carpal tunnel dimensions along anatomically defined axes in the radio-ulnar and dorso-palmar directions (Cobb et al., 1993, Kamolz et al., 2001, Kamolz et al., 2004, Lee et al., 2005, Lee et al., 1999, Liang, 1987, Sora and Genser-Strobl, 2005). However, the carpal tunnel has been indicated as an elliptical shape that is oriented obliquely with respect to the anatomical axes (Mogk and Keir, 2008, Pacek et al., 2010, Robbins, 1963). Therefore, the major axis of the carpal tunnel is not aligned with the standard anatomically defined directions. Mogk and Keir (2008) measured the largest width and depth of the oblique carpal tunnel, but the orientation of the tunnel was not reported. Pacek et al. (2010) reported elliptical dimensions of the carpal tunnel, including the tilt angle of the ellipse, but did not differentiate the dimensions of the distal carpal tunnel.

The distal carpal tunnel at the hook of the hamate is clinically pertinent because it is a common site for median nerve compression (Buchberger et al., 1991, Mesgarzadeh et al., 1989b) due to regional stenosis (Dekel et al., 1980), structural stiffening (Xiu et al., 2010), and pressure elevation (Goss and Agee, 2010, Mesgarzadeh et al., 1995). Therefore, the main purpose of this study is to investigate the morphometric characteristics (e.g. elliptical properties) of the distal carpal tunnel and its surrounding structures. A secondary purpose is to examine the relationships among the morphological parameters.

3 Materials and Methods

Morphometric analyses were performed on the cross section at distal carpal tunnel aligned with the hook of hamate. The magnetic resonance (MR) imaging data used in this study was a part of our previous study for an investigation of the relationship between carpal tunnel pressure and tunnel cross-sectional area (Li et al., 2011). Briefly, MR imaging data were collected from eight cadaveric specimens (mean age of 47.4 years, 42–55 years) with no previously documented injury or surgery to the wrist. Upon dissection preparation, a

medical balloon filled with a contrast agent was inserted into an evacuated carpal tunnel to apply a nominal pressure of 10 mmHg (Fig. 1).

Each MR image was analyzed using *ImageJ* (v1.43, National Institutes of Health, USA) to obtain morphological parameters of the carpal tunnel (Fig. 2). The polygon selection tool was used to outline (1) the balloon boundary (i.e. carpal tunnel), (2) the interior carpus boundary, and (3) the exterior carpus boundary (Fig. 1). The balloon boundary, in combination with a convex hull technique, served as the boundary of the carpal tunnel. The convex hull technique aided in reconstruction of the boundary with a smooth envelope that removed cavities caused by the wrinkles in the balloon. The interior carpus boundary included the carpal tunnel but extended, primarily in the dorsal and radial directions, to the interior boundary of the carpal bones to include the intercarpal ligaments (Gabra and Li, 2013). The exterior carpus boundary extended to the exterior boundary of the carpal bones, including the carpal tunnel, intercarpal ligaments, and the carpal bones.

Several morphological outcomes were derived from each boundary, including area, perimeter, and fit ellipse parameters (i.e. major axis length, minor axis length, aspect ratio, and orientation) (Fig. 2). Orientation of a boundary was measured by the pronation angle, which is defined as the angle between the major axis and the hamate-trapezium axis (i.e. a line connecting the most volar aspects of the hook of the hamate and the ridge of the trapezium). The carpal arch width (CAW) was defined as the distance between the hook of hamate and the ridge of the trapezium. Then, the midpoint between the CAW endpoints was identified along the hamate-trapezium axis, and the carpal arch height (CAH) was determined as the perpendicular distance from this midpoint to the dorsal border of the TCL.

A one-way repeated-measures ANOVA was performed to compare the carpal tunnel, interior carpus boundary, and the exterior carpus boundary for each outcome parameter (area, perimeter, major axis length, minor axis length, aspect ratio, pronation angle). A repeated-measures ANOVA on ranks was performed for those parameters that failed equal variance testing. Spearman Rank Order correlation and linear regression analyses were performed to determine the relationship between the CAW and each parameter. A p-value less than 0.05 was considered statistically significant.

4 Results

The eight specimens (n = 8) had an average carpal arch width (CAW) of 23.9 ± 2.9 mm and a carpal arch height (CAH) of 2.2 ± 0.9 mm. The cross-sectional areas formed by the carpal tunnel, interior carpus boundary, and exterior carpus boundary were 183.5 ± 30.1 mm^2, 240.7 ± 40.2 mm^2, and 1002.3 ± 183.7 mm^2, respectively. The exterior carpus boundary had a significantly larger area than both the interior carpus and carpal tunnel boundaries ($p < 0.001$). More specifically, the area of the exterior carpus boundary was 5.5 and 4.2 times those of the carpal tunnel and interior carpus boundary, respectively. The perimeters of the carpal tunnel, interior carpus and exterior carpus boundaries were 54.8 ± 4.5 mm, 68.5 ± 7.0 mm, and 130.6 ± 11.8 mm, respectively, and they were significantly different from one another ($p < 0.001$). The perimeters of the carpal tunnel and interior carpus boundaries significantly correlated with the CAW (Table 1, Figure 3).

The major axis length of the carpal tunnel boundary elliptic fit was 21.3 ± 1.8 mm while that of the interior carpus boundary was 24.4 ± 2.4 mm. The exterior carpus boundary major axis length, 47.2 ± 5.0 mm, was significantly larger than those of the carpal tunnel and interior carpus boundary ($p < 0.05$) (Fig. 4). The major axis lengths of the carpal tunnel and the interior carpus correlated ($p < 0.05$) with CAW (Table 1) (Fig. 5). The minor axis lengths of the carpal tunnel (10.9 ± 1.1 mm), interior carpus boundary (12.5 ± 1.2 mm), and exterior carpus boundary (26.9 ± 2.7 mm) were significantly different from each other ($p < 0.05$) (Fig. 4). The aspect ratios of the carpal tunnel, interior carpus and exterior carpus boundaries were 1.96 ± 0.15, 1.96 ± 0.19, and 1.76 ± 0.19, respectively. The aspect ratios of the carpal tunnel and interior carpus boundaries were not significantly different from each other ($p > 0.05$), but they were significantly greater (i.e. more elliptic) than that of the exterior carpus boundary ($p < 0.001$). The carpal tunnel's major axis was pronated, relative to hamate-trapezium axis, by 15.9 ± 2.2°, which was significantly greater than the pronation angles of the interior carpus boundary (8.2 ± 3.2°) and exterior carpus boundary (6.0 ± 3.0°) ($p < 0.001$).

5 Discussion

Cross-sectional images at the carpal tunnel's distal boundary were analyzed because it is a common site for median nerve compression (Buchberger et al., 1991, Mesgarzadeh et al., 1989b). The carpal tunnel boundary was accurately delineated on the magnetic resonance images by the pressurized medical balloon. We also defined the boundaries formed by the interior and exterior borders of carpal bones. The interior boundary was analyzed because previous studies have used this boundary to determine the carpal tunnel's cross-sectional area (Dekel et al., 1980, Monagle et al., 1999, Papaioannou et al., 1992) even though it includes soft tissues that are separate from the carpal tunnel (Gabra and Li, 2013). The exterior carpus boundary aided in size comparisons between the carpal tunnel and the surrounding carpus. Morphometric parameters were derived from and compared among the three boundaries.

Carpal tunnel morphometry can assist in identifying and evaluating abnormalities. For example, carpal arch height (CAH) is an indicator for the palmar bowing of the TCL (Buchberger et al., 1991, Buchberger et al., 1992, Mesgarzadeh et al., 1989a, Mesgarzadeh et al., 1989b, Monagle et al., 1999), which may be due to a high carpal tunnel pressure (Kim et al., 2013, Li et al., 2011, Zagnoli et al., 1999). Studies have shown that patients with carpal tunnel syndrome have an increased carpal arch height compared to healthy individuals. The CAH data from the current study (2.2 mm) agrees well with previous studies of normative populations (1.9–2.7 mm) (Allmann et al., 1997, Buchberger et al., 1991, Monagle et al., 1999). To normalize the CAH, Mesgarzadeh et al. (1989a) reported a carpal arch bowing ratio (i.e. CAH/CAW) of 5.8%. The corresponding bowing ratio of the current study is 9.2% (= 2.2/23.9) with a standard deviation of 3.8% agrees with the *in vivo* data of Mesgarzadeh et al. (1989a). This provided support, as well as justification, that the pressurized medical balloon simulated the physiological pressure of the carpal tunnel in maintaining an arched TCL.

Relative to the surrounding carpus, the carpal tunnel is considerably smaller in size. More specifically, the tunnel's area is 18% (=183.5/1002.3) of the cross-sectional area of the exterior carpus boundary. The interior carpus boundary is 57 mm^2 greater than that of the tunnel area and it is attributed to the soft tissues (e.g. intercarpal ligaments and flexor carpi radialis tendon) that abut the carpal tunnel on its ulnar, dorsal, and radial sides (Gabra and Li, 2013). The interior carpus boundary occupies 24% of the exterior carpus boundary area. The area difference between the exterior carpus boundary and interior carpus boundary (762 mm^2) accounts for the area occupied by the hamate, capitate, trapezoid, trapezium, and their intercarpal ligaments. Likewise, the exterior carpus boundary has the largest perimeter and the carpal tunnel has the smallest perimeter. The carpal tunnel perimeter of 54.8 mm agrees with previous studies that reported this parameter for the carpal tunnel (52.3–54.9 mm) (Kamolz et al., 2001, Mogk and Keir, 2008). The perimeters of the carpal tunnel and interior carpal boundary are 42% (= 54.8/130.6) and 52% (= 68.5/130.6), respectively, of the exterior carpus boundary's perimeter. Such comparative measurements of the areas or perimeters among the boundaries is useful in identifying morphological changes caused by pathologies such as callus formations (e.g. osteopetrosis), bone fractures, dislocations, deformity, and malalignment of the carpal bones (Mesgarzadeh et al., 1989b, Rakic et al., 1986, Schnetzler, 2008). The current study determined that the perimeters of the carpal tunnel and interior carpus boundary are strongly correlated with the CAW. Thus, the CAW-perimeter relationships provide a method for estimating the respective perimeter when the boundaries are not easily visualized in certain imaging modalities, such as ultrasound and radiography.

The carpal tunnel, interior carpus boundary, and exterior carpus boundary were elliptical in shape, which are quantified by geometrical parameters of the major axis length, minor axis length, aspect ratio, and pronation angle. Previous studies examined the radio-ulnar and dorso-volar diameters of the carpal tunnel aligned with anatomical axes without consideration of the tunnel's oblique orientation (Cobb et al., 1993, Kamolz et al., 2001, Kamolz et al., 2004, Lee et al., 2005, Lee et al., 1999, Liang, 1987, Sora and Genser-Strobl, 2005). The advantage of deriving the major and minor axes from a fit ellipse is that the axes are intrinsic properties of the shape, which are invariant to defined coordinate systems.

From the fit ellipse analysis, the major axis increased sequentially for the carpal tunnel, interior carpus boundary, and exterior carpus boundary. The interior carpus boundary has larger major axis than that of the carpal tunnel because of inclusion of flexor carpi radialis tendon, and the increased major axis of the exterior carpus boundary is due to the width of the carpal bones, primarily the hamate and trapezium. We also found that the major axis of the carpal tunnel and interior carpus boundary strongly correlated with the CAW, which corroborates with a previous study showing a strong correlation between the carpal tunnel major axis length and the width of the palm (Pacek et al., 2010). However, the width of the palm can be affected by soft tissues and thus a wider palm, due to fatty tissue, may not mean a wider carpal tunnel. The CAW is determined from osseous landmarks and therefore eliminates the influence of soft tissues for prediction of the major axes of the carpal tunnel and interior carpus boundary.

The minor axis length of the carpal tunnel could be used for identifying aberrant changes to the carpal tunnel and for surgical planning. For example, a decrease in the carpal tunnel's minor axis length could be due to fat development on the capitate-trapezium ligament (Mesgarzadeh et al., 1989a). The minor axis of the carpal tunnel is also an indicator of the carpal tunnel's depth to determine the technique of carpal tunnel release. An endoscopic trocar that is larger than the tunnel depth may increase the risk of injury to the median nerve during endoscopic carpal tunnel release, and therefore indicates the use of an open carpal tunnel release technique (Kamolz et al., 2001). Similar to the trend of other parameters, the minor axis increased sequentially for the carpal tunnel, interior carpus boundary, and exterior carpus boundary, respectively. The minor axis of the interior carpus boundary is larger than that of the carpal tunnel due to the palmar intercarpal ligaments (Gabra and Li, 2013).

The aspect ratio was calculated as the ratio of the major axis to the minor axis, quantifying the extent of non-circularity. A minimum aspect ratio of 1 indicates a circular shape, while a greater aspect ratio indicates a more elliptical shape. A previous study reported the roundness (i.e. inverse of the aspect ratio) of the carpal tunnel as 0.474 (Mogk and Keir, 2008), which is consistent with the current finding of a roundness value of 0.51 (= 1/1.96). Interestingly, previous studies have suggested a link between carpal tunnel syndrome and the aspect ratio of the carpal tunnel (Kamolz et al., 2004, Mogk and Keir, 2008). Kamolz et al. (2004) showed that persons with carpal tunnel syndrome have rounder carpal tunnels, i.e. smaller aspect ratio, than healthy controls, which may be explained by the increased CAH (Buchberger et al., 1991, Buchberger et al., 1992, Mesgarzadeh et al., 1989b, Mogk and Keir, 2008, Monagle et al., 1999).

We found that the major axes of the carpal tunnel, interior carpus boundary, and exterior carpus boundary were oblique to the hamate-trapezium axis. Among the three boundaries, the carpal tunnel has the greatest pronation angle (15.9°), followed by the interior carpus boundary (8.2°) and exterior carpus boundary (6.0°). In a previous study using a silicon molding and digitization technique, Pacek et al. (2010) also reported tilt angles of the carpal tunnel, progressively increasing from 8° at the proximal level to 16° at the distal level. The pronation angle (15.9°) of the carpal tunnel at the hamate level in this study is in agreement with the findings of Pacek et al. (2010). In a study by Mogk and Keir (2008), the pronation angle of the carpal tunnel was not explicitly quantified, but the authors made the observation that the carpal tunnel was pronated from the anatomical axes by approximately 30°. This observation (Mogk and Keir, 2008) is also in agreement with the results of the current study. This is because the hook of the hamate is generally more dorsal than the ridge of the trapezium causing the hamate-trapezium axis to have some degree of pronation relative to the surface-based anatomical radio-ulnar axis. Given that the pronation angle in the current study was quantified with respect to the hamate-trapezium axis, the carpal tunnel is even more pronated relative to the radio-ulnar axis based on surface anatomy.

The oblique orientation of the carpal tunnel may help explain functional kinematics of the wrist related to the dart-thrower's motion (Li et al., 2005, Moritomo et al., 2007, Palmer et al., 1985, Werner et al., 2004). In many functional tasks of the hand, the wrist has a tendency of angular motion from radial-extension to ulnar-flexion, i.e. dart-thrower's

motion, around an oblique axis of rotation (Capener, 1956, Fisk, 1981, Li et al., 2005, Moritomo et al., 2007, Palmer et al., 1985). The pronated major axis of the carpal tunnel determined in the current study may be in alignment of the rotational axis of the dart-thrower's motion of the wrist. Several factors such as ligament constraints, bony configuration, and muscle actions have been ascribed to the dart thrower's motion (Capener, 1956, Moritomo et al., 2007, Saffar and Semaan, 1994), but carpal tunnel morphology may also be implicated to dart-thrower's motion. Furthermore, the oblique orientation of the carpal tunnel may also be associated with the oblique orientation of the wrist's mechanical axes. For example, the stiffness profile of the wrist has a major axis that is oriented −69° from the directions of pure flexion (volarly) and extension (dorsally) meaning that it is "pronated" 21° from the radial-ulnar axis (Crisco et al., 2011). Thus, the carpal tunnel's major axis is similarly pronated as that of the wrist's stiffness profile.

Generally, the morphological parameters among the three boundaries were correlated with each other (Table 1). Interestingly, 7 of the 9 pairs between the carpal tunnel and interior carpus boundary had high correlation coefficients, which can be explained by their proximity in size and shape of the two boundaries. In contrast, only 4 of the 9 pairs had high correlation coefficients between the interior and exterior carpus boundaries. Morphological parameters of the carpal tunnel are not strongly correlated with those of the exterior carpus boundary. This indicates that the shapes of these two boundaries are not uniformly scaled, due to the fact that the carpal bones situate on the dorsal aspects of the carpal tunnel.

We acknowledge a few limitations in this study. One limitation is that morphometry was not performed on the skin/surface boundary of the wrist due to the dissection of the tissues for the insertion and positioning of the pressurized medical balloon in the carpal tunnel to mimic a physiological pressure condition in cadaveric hands. The dissection disrupted the tissue structure volar to the transverse carpal ligament, but should have little influence on the carpal tunnel that is dorsal to the transverse carpal ligament. Another limitation is that the findings reported in this study are based on the distal level of the carpal tunnel and they may not be applicable to other levels along the tunnel. Future studies are needed to characterize the three-dimensional morphological anatomy of the tunnel by including the entire tunnel length. Lastly, the measurements presented in this study are pertinent to a normative population. These findings could be affected by pathologies of the carpal tunnel and wrist, and future studies can determine the pathological changes to the carpal tunnel morphology.

In summary, we have investigated the morphological properties of the carpal tunnel and its neighboring structures. The cross-sectional area of the tunnel, at the level of hamate level, is less than 20% of the area enclosed by the carpal bones. The carpal tunnel's cross-section is elliptical in shape with a major axis that is twice as large as its minor axis. Furthermore, the tunnel's cross section is obliquely oriented with its major axis pronated with respect to the anatomical radio-ulnar axis. The interior and exterior carpus boundaries also had elliptical cross-sections. The results of the morphological properties of the carpal tunnel and its surrounding configuration enhance our understanding of carpal tunnel structure and function for clinical applications.

Acknowledgements

The authors thank Tamara Marquardt for collecting the imaging data and Suk Yu for assistance with image analysis. This publication was made possible by Grant Number R21AR062753 from NIAMS/NIH. Its contents are solely the responsibility of the authors and do not necessarily represent the official views of the NIAMS or NIH. The authors would also like to recognize those who graciously donated themselves to enable this research.

References

Ablove RH, Peimer CA, Diao E, Oliverio R, Kuhn JP. Morphologic changes following endoscopic and two-portal subcutaneous carpal tunnel release. J Hand Surg Am. 1994; 19:821–826. [PubMed: 7806811]

Allmann KH, Horch R, Uhl M, Gufler H, Altehoefer C, Stark GB, Langer M. MR imaging of the carpal tunnel. Eur J Radiol. 1997; 25:141–145. [PubMed: 9283842]

Bleecker ML, Bohlman M, Moreland R, Tipton A. Carpal tunnel syndrome: role of carpal canal size. Neurology. 1985; 35:1599–1604. [PubMed: 4058749]

Brahme SK, Hodler J, Braun RM, Sebrechts C, Jackson W, Resnick D. Dynamic MR imaging of carpal tunnel syndrome. Skeletal Radiol. 1997; 26:482–487. [PubMed: 9297753]

Buchberger W, Schon G, Strasser K, Jungwirth W. High-resolution ultrasonography of the carpal tunnel. J Ultrasound Med. 1991; 10:531–537. [PubMed: 1942218]

Buchberger W, Judmaier W, Birbamer G, Lener M, Schmidauer C. Carpal tunnel syndrome: diagnosis with high-resolution sonography. AJR Am J Roentgenol. 1992; 159:793–798. [PubMed: 1529845]

Capener N. The hand in surgery. J Bone Joint Surg Br. 1956; 38-B:128–151. [PubMed: 13295325]

Cho MS, Means KR, Shrout JA, Segalman KA. Carpal tunnel volume changes of the wrist under distraction. J Hand Surg Eur Vol. 2008; 33:648–652. [PubMed: 18977835]

Chroni E, Paschalis C, Arvaniti C, Zotou K, Nikolakopoulou A, Papapetropoulos T. Carpal tunnel syndrome and hand configuration. Muscle Nerve. 2001; 24:1607–1611. [PubMed: 11745969]

Cobb TK, Dalley BK, Posteraro RH, Lewis RC. Anatomy of the flexor retinaculum. J Hand Surg Am. 1993; 18:91–99. [PubMed: 8423326]

Crisco JJ, Heard WM, Rich RR, Paller DJ, Wolfe SW. The mechanical axes of the wrist are oriented obliquely to the anatomical axes. J Bone Joint Surg Am. 2011; 93:169–177. [PubMed: 21248214]

Dekel S, Papaioannou T, Rushworth G, Coates R. Idiopathic carpal tunnel syndrome caused by carpal stenosis. Br Med J. 1980; 280:1297–1299. [PubMed: 7388516]

Fisk, G. Biomechanics of the Wrist Joint. In: Tubiana, R., editor. The Hand. Philadelphia: W.B. Saunders; 1981. p. 136-141.

Gabra JN, Li ZM. Carpal Tunnel Cross-Sectional Area Affected by Soft Tissues Abutting the Carpal Bones. J Wrist Surg. 2013; 2:73–78. [PubMed: 23607081]

Gordon C, Johnson EW, Gatens PF, Ashton JJ. Wrist ratio correlation with carpal tunnel syndrome in industry. Am J Phys Med Rehabil. 1988; 67:270–272. [PubMed: 3196452]

Goss BC, Agee JM. Dynamics of intracarpal tunnel pressure in patients with carpal tunnel syndrome. J Hand Surg Am. 2010; 35:197–206. [PubMed: 20022712]

Healy C, Watson JD, Longstaff A, Campbell MJ. Magnetic resonance imaging of the carpal tunnel. J Hand Surg Br. 1990; 15:243–248. [PubMed: 2366024]

Kamolz LP, Schrogendorfer KF, Rab M, Girsch W, Gruber H, Frey M. The precision of ultrasound imaging and its relevance for carpal tunnel syndrome. Surg Radiol Anat. 2001; 23:117–121. [PubMed: 11462859]

Kamolz LP, Beck H, Haslik W, Hogler R, Rab M, Schrogendorfer KF, Frey M. Carpal tunnel syndrome: a question of hand and wrist configurations? J Hand Surg Br. 2004; 29:321–324. [PubMed: 15234493]

Kato T, Kuroshima N, Okutsu I, Ninomiya S. Effects of endoscopic release of the transverse carpal ligament on carpal canal volume. J Hand Surg Am. 1994; 19:416–419. [PubMed: 8056968]

Kim DH, Marquardt TL, Gabra JN, Shen ZL, Evans PJ, Seitz WH, Li ZM. Pressure-morphology relationship of a released carpal tunnel. J Orthop Res. 2013; 31:616–620. [PubMed: 23184493]

Lee CH, Kim TK, Yoon ES, Dhong ES. Postoperative morphologic analysis of carpal tunnel syndrome using high-resolution ultrasonography. Ann Plast Surg. 2005; 54:143–146. [PubMed: 15655463]

Lee D, Van holsbeeck MT, Janevski PK, Ganos DL, Ditmars DM, Darian VB. Diagnosis of carpal tunnel syndrome. Ultrasound versus electromyography. Radiol Clin North Am. 1999; 37:859–872. x. [PubMed: 10442084]

Li ZM, Kuxhaus L, Fisk JA, Christophel TH. Coupling between wrist flexion-extension and radial-ulnar deviation. Clin Biomech (Bristol, Avon). 2005; 20:177–183.

Li ZM, Masters TL, Mondello TA. Area and shape changes of the carpal tunnel in response to tunnel pressure. J Orthop Res. 2011; 29:1951–1956. [PubMed: 21608024]

Liang CL. CT-scanning study of cross-sectional area of the carpal tunnel in cases of carpal tunnel syndrome. Nihon Seikeigeka Gakkai Zasshi. 1987; 61:1033–1045. [PubMed: 3437172]

Mesgarzadeh M, Schneck CD, Bonakdarpour A. Carpal tunnel: MR imaging. Part I. Normal anatomy. Radiology. 1989a; 171:743–748. [PubMed: 2717746]

Mesgarzadeh M, Schneck CD, Bonakdarpour A, Mitra A, Conaway D. Carpal tunnel: MR imaging. Part II. Carpal tunnel syndrome. Radiology. 1989b; 171:749–754. [PubMed: 2541464]

Mesgarzadeh M, Triolo J, Schneck CD. Carpal tunnel syndrome. MR imaging diagnosis. Magn Reson Imaging Clin N Am. 1995; 3:249–264. [PubMed: 7553021]

Mogk JP, Keir PJ. Wrist and carpal tunnel size and shape measurements: effects of posture. Clin Biomech (Bristol, Avon). 2008; 23:1112–1120.

Monagle K, Dai G, Chu A, Burnham RS, Snyder RE. Quantitative MR imaging of carpal tunnel syndrome. AJR Am J Roentgenol. 1999; 172:1581–1586. [PubMed: 10350293]

Moritomo H, Apergis EP, Herzberg G, Werner FW, Wolfe SW, Garcia-elias M. 2007 IFSSH committee report of wrist biomechanics committee: biomechanics of the so-called dart-throwing motion of the wrist. J Hand Surg Am. 2007; 32:1447–1453. [PubMed: 17996783]

Pacek CA, Tang J, Goitz RJ, Kaufmann RA, Li ZM. Morphological analysis of the carpal tunnel. Hand (N Y). 2010; 5:77–81. [PubMed: 19760464]

Palmer AK, Werner FW, Murphy D, Glisson R. Functional wrist motion: a biomechanical study. J Hand Surg Am. 1985; 10:39–46. [PubMed: 3968403]

Papaioannou T, Rushworth G, Atar D, Dekel S. Carpal canal stenosis in men with idiopathic carpal tunnel syndrome. Clin Orthop Relat Res. 1992:210–213. [PubMed: 1446439]

Radecki P. A gender specific wrist ratio and the likelihood of a median nerve abnormality at the carpal tunnel. Am J Phys Med Rehabil. 1994; 73:157–162. [PubMed: 8198771]

Rakic M, Elhosseiny A, Ramadan F, Iyer R, Howard RG, Gross L. Adult-type osteopetrosis presenting as carpal tunnel syndrome. Arthritis Rheum. 1986; 29:926–928. [PubMed: 3741505]

Richman JA, Gelberman RH, Rydevik BL, Hajek PC, Braun RM, Gylys-morin VM, Berthoty D. Carpal tunnel syndrome: morphologic changes after release of the transverse carpal ligament. J Hand Surg Am. 1989; 14:852–857. [PubMed: 2794405]

Robbins H. Anatomical Study of the Median Nerve in the Carpal Tunnel and Etiologies of the Carpal-Tunnel Syndrome. J Bone Joint Surg Am. 1963; 45:953–966. [PubMed: 14047366]

Saffar, P.; Semaan, I. The Study of the Biomechanics of Wrist Movements in an Oblique Plane — A Preliminary Report. In: Schuind, F.; An, KN.; Cooney, WP., III; Garcia-elias, M., editors. Advances in the Biomechanics of the Hand and Wrist. Springer: 1994. p. 305-311.

Schnetzler KA. Acute carpal tunnel syndrome. J Am Acad Orthop Surg. 2008; 16:276–282. [PubMed: 18460688]

Sora MC, Genser-strobl B. The sectional anatomy of the carpal tunnel and its related neurovascular structures studied by using plastination. Eur J Neurol. 2005; 12:380–384. [PubMed: 15804269]

Werner FW, Green JK, Short WH, Masaoka S. Scaphoid and lunate motion during a wrist dart throw motion. J Hand Surg Am. 2004; 29:418–422. [PubMed: 15140483]

Xiu KH, Kim JH, Li ZM. Biomechanics of the transverse carpal arch under carpal bone loading. Clin Biomech (Bristol, Avon). 2010; 25:776–780.

Zagnoli F, Andre V, Le dreff P, Garcia JF, Bellard S. Idiopathic carpal tunnel syndrome. Clinical, electrodiagnostic, and magnetic resonance imaging correlations. Rev Rhum Engl Ed. 1999; 66:192–200. [PubMed: 10339774]

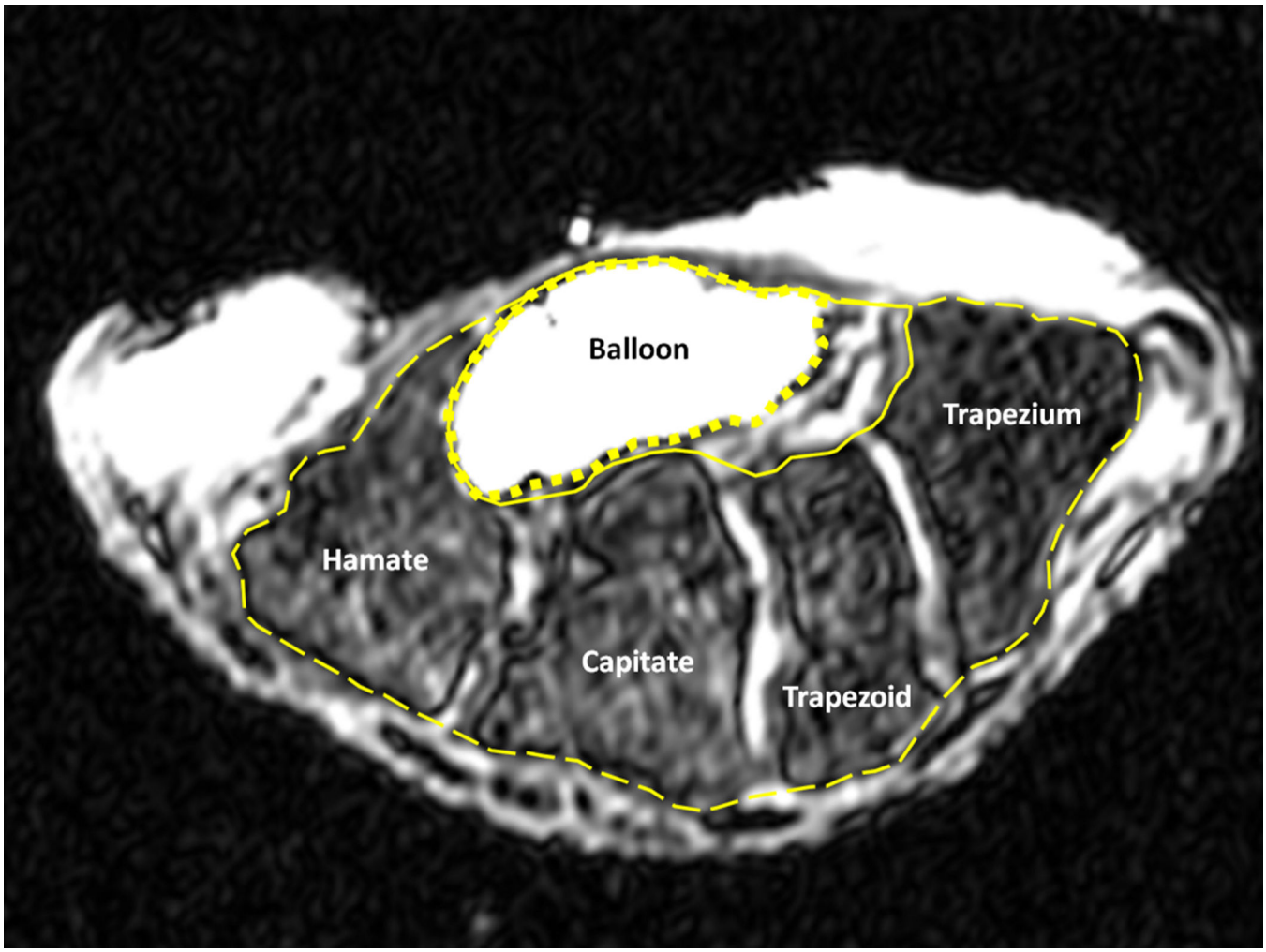

Figure 1.
A representative magnetic resonance (MR) image of the carpal tunnel at the level of the hook of the hamate and the ridge of the trapezium displaying the balloon (i.e. carpal tunnel) boundary (dotted line), interior carpus boundary (solid line), and exterior carpus boundary (dashed line).

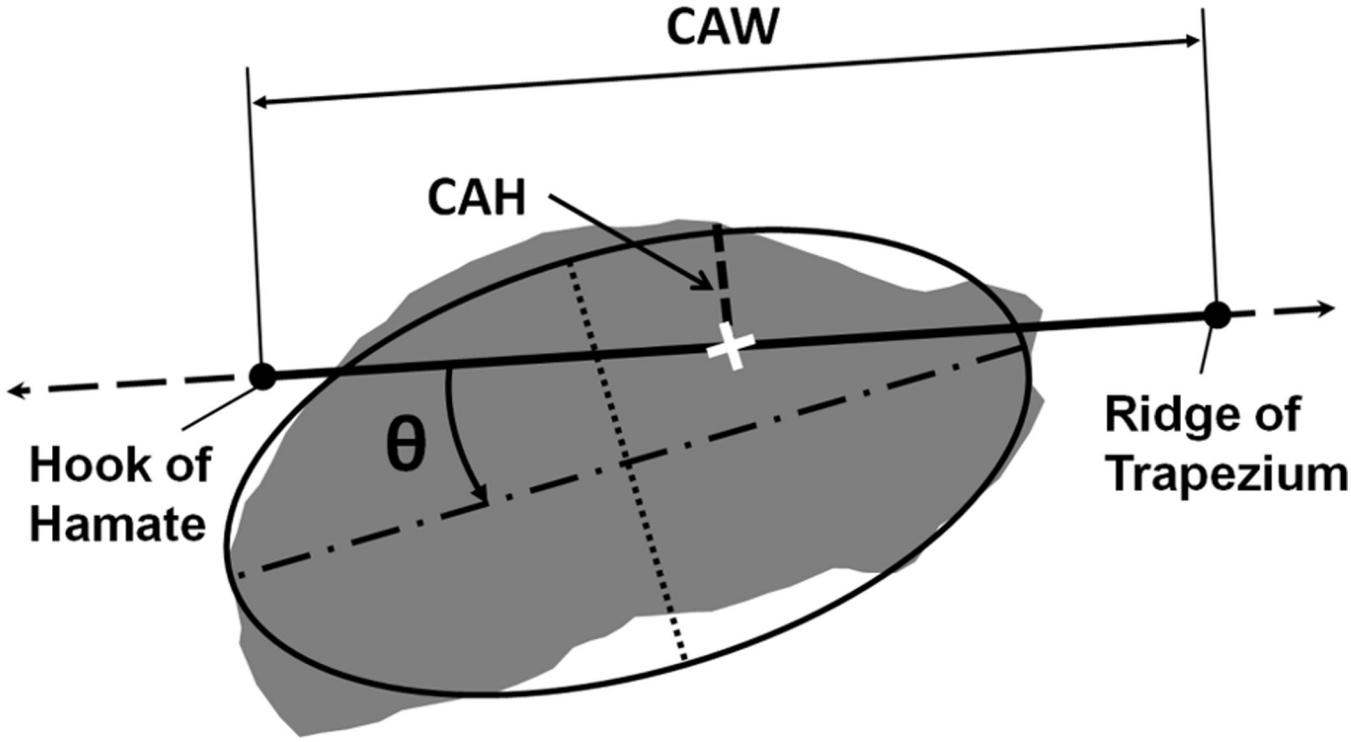

Figure 2.

Morphological parameters of the carpal tunnel. Shown are the morphological parameters for carpal arch width (CAW, solid line with endpoints), carpal arch height (CAH, dashed line), cross-sectional area (shaded region), and perimeter (outline of shaded region) with elliptical fit parameters such as major axis length (dashed dot line), minor axis length (dotted line), and pronation angle (θ) relative to the hamate-trapezium axis (dashed line with arrows).

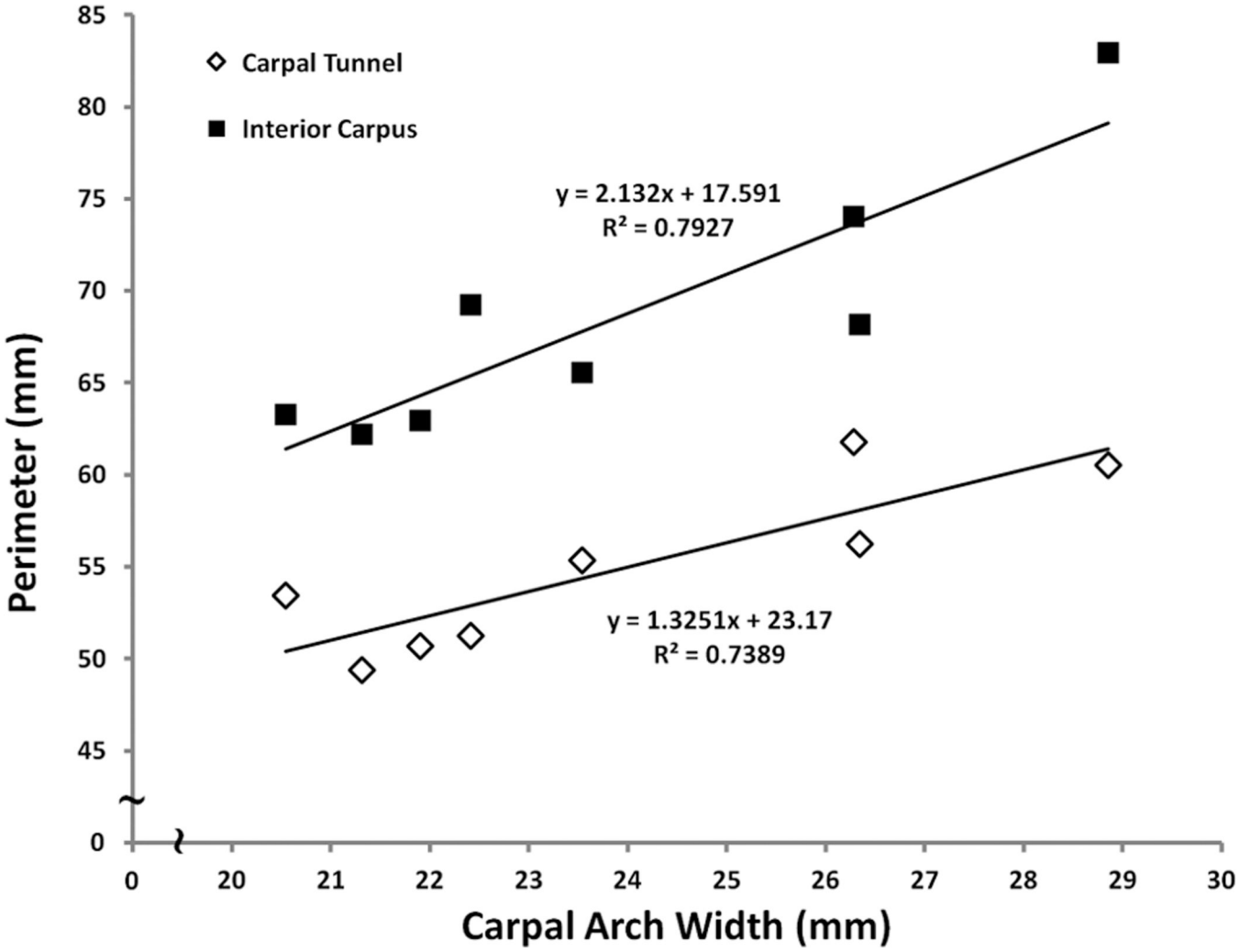

Figure 3.
Linear regression analysis of perimeter as a function of carpal arch width (CAW) for the carpal tunnel and interior carpus boundary.

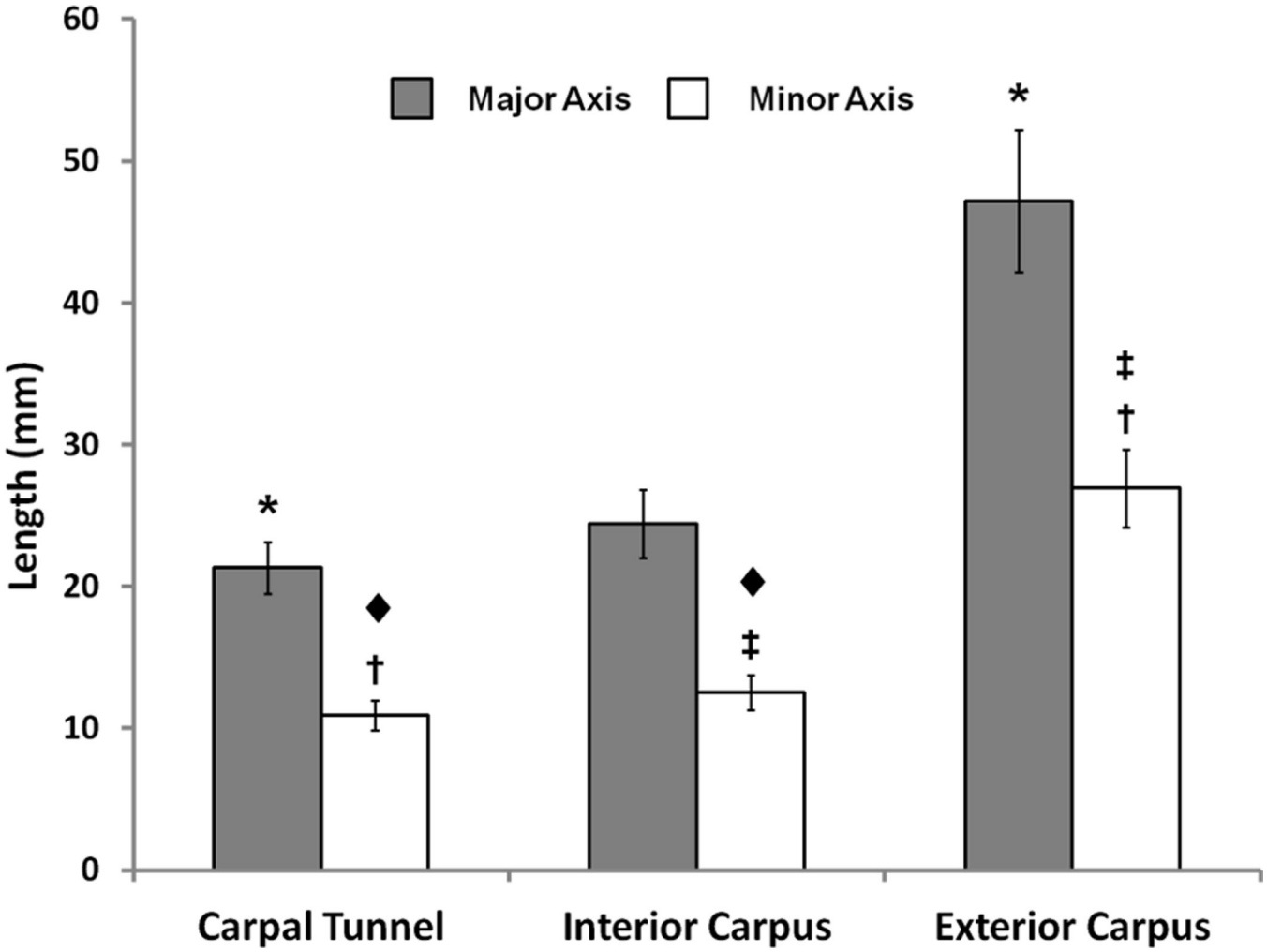

Figure 4.

The mean and standard deviation of major and minor axes length with statistical results for the carpal tunnel, interior carpus boundary, and exterior carpus boundary (* and ◆ denote $p < 0.05$; † and ‡ denote $p < 0.001$).

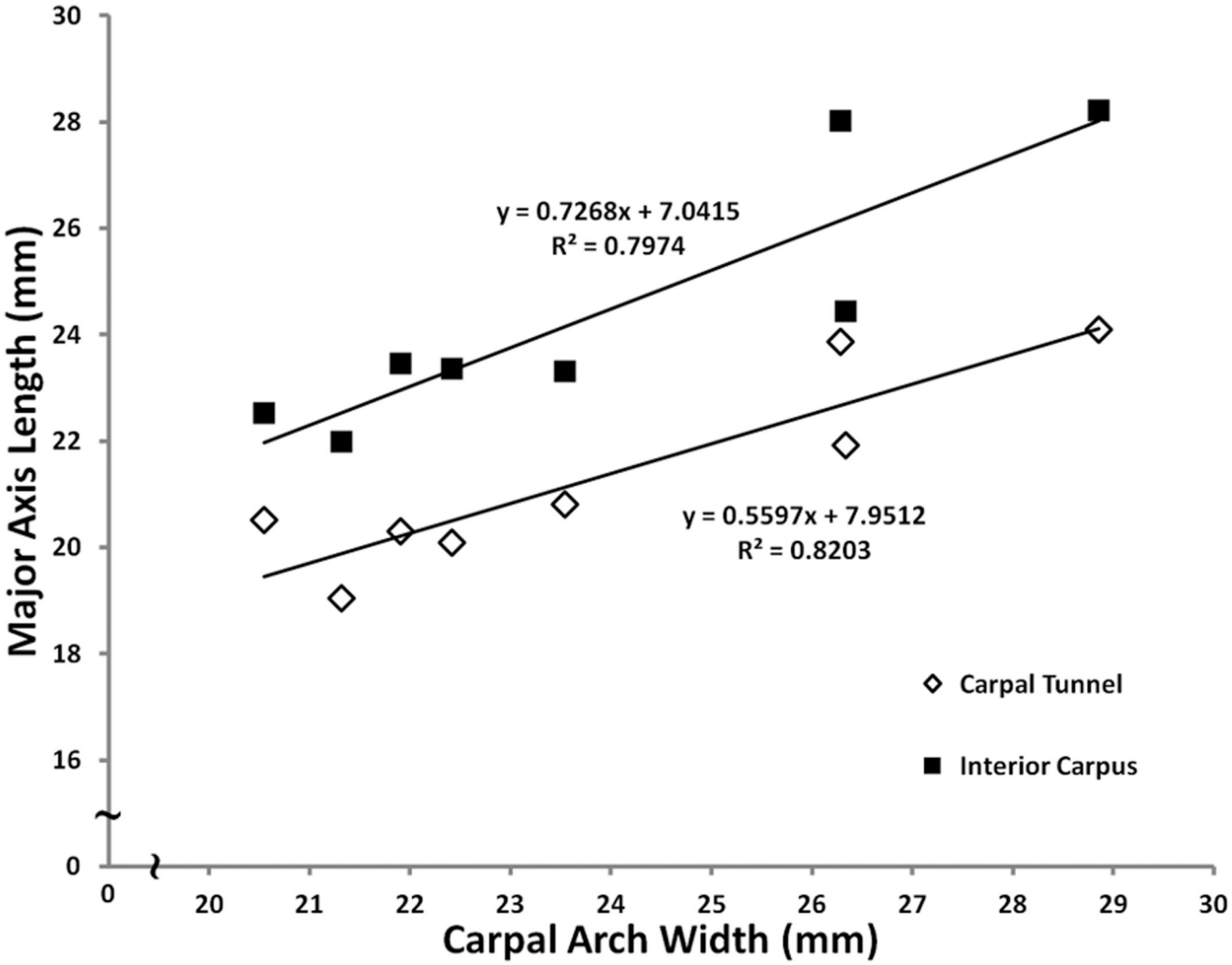

Figure 5.
Linear regression analysis of major axis length as a function of carpal arch width (CAW) for the carpal tunnel and interior carpus boundary.

Table 1

Spearman Rank Order Correlation Coefficients among the morphological parameters

			Carpal Tunnel			Interior carpus			Exterior carpus		
		CAW	**Perimeter**	**Major**	**Minor**	**Perimeter**	**Major**	**Minor**	**Perimeter**	**Major**	**Minor**
Carpal Tunnel	Perimeter	0.786*									
	Major	0.810*	0.952*								
	Minor	0.619	0.690*	0.762*							
Interior carpus	Perimeter	0.810*	0.833*	0.762*	0.333						
	Major	0.857*	0.762*	0.810*	0.381	0.810*					
	Minor	0.310	0.714*	0.690*	0.762*	0.381	0.262				
Exterior	Perimeter	0.452	0.548	0.548	0.071	0.667	0.738*	0.381			
	Major	0.571	0.429	0.429	−0.190	0.714*	0.810*	−0.167	0.738*		
	Minor	0.476	0.881*	0.881*	0.595	0.643	0.595	0.833*	0.619	0.310	

*p<0.05